

# Bile pigment complexes with cyclodextrins: electronic and vibrational circular dichroism study

Iryna Goncharova<sup>a</sup> and Marie Urbanová<sup>b,\*</sup>

<sup>a</sup>Department of Analytical Chemistry, Institute of Chemical Technology, Prague, Technická 5, 166 28 Prague 6, Czech Republic

<sup>b</sup>Department of Physics and Measurements, Institute of Chemical Technology, Prague, Technická 5, 166 28 Prague 6, Czech Republic

Received 4 July 2007; accepted 20 August 2007

**Abstract**—Chiral recognition of bilirubin IX- $\alpha$ , biliverdin IX- $\alpha$ , and bilirubin ditaurate dianions by cyclodextrins was studied using a combination of vibrational and electronic circular dichroism. Biliverdin forms inclusion complexes with  $\beta$ -cyclodextrin and  $\beta$ -methylcyclodextrin. Bilirubin bonds to both cyclodextrins by means of hydrogen bonds and only shallow inclusions that are restricted by the presence of COO<sup>-</sup> in the pigment structure. Bilirubin ditaurate complexes are realized by a weak inclusion of the whole molecule, or some part of it, into the cyclodextrin cavity and stabilization of the conformation by hydrogen bonds. Bilirubin and bilirubin ditaurate can be recognized by cyclodextrin and methylcyclodextrin in the form of opposite conformers. Spectroscopic characteristics of the different conformations of the bile pigments were obtained for the first time by vibrational circular dichroism techniques.

© 2007 Elsevier Ltd. All rights reserved.

## 1. Introduction

Heme, the prosthetic group of hemoglobin and other mammalian heme proteins, is degraded by oxidation in the spleen to produce biliverdin IX- $\alpha$ . Biliverdin (BV) undergoes reduction at the methylene bridge to form bilirubin IX- $\alpha$  (BR). Although the chemical structures of these bile pigments are very similar, their solution conformations differ greatly. The structures are closely approximated in Figure 1. In BR intramolecular hydrogen bonding occurs between the carboxylic acid groups of the propionate side chains and the lactam and pyrrole groups of the opposite dipyrrole units. The extent of hydrogen bonding in aqueous solutions at physiological pH is currently under debate, but it is well established that BR adopts this ‘ridge-tile’ conformation<sup>1–4</sup> where the planes of the two dipyrrole units are at an angle of 95–100°. This structure is stabilized by six hydrogen bonds in the case of the diacidic form of the pigment. In contrast, BV adopts a helical ‘lock-washer’ conformation (helices like chiral ‘clamps’) in aqueous solution.<sup>2,5–9</sup> The helical inversion equilibrium between the two enantiomeric helices M and P (Fig. 1) is typical for these pigments in solution. Both BR and BV are poorly soluble in water at physiologic pH (~70 ng) and their transporta-

tion into the liver occurs in the form of a noncovalent complex with serum albumin. BR is esterified with *o*-glucuronic acid in the liver prior to excretion. Conjugation of the sugar moieties prevents the formation of intramolecular hydrogen bonds and renders conjugated BR water-soluble. Bilirubin glucuronides are reactive, undergoing acyl migration and facile hydrolysis, and they are not readily available. In contrast, bilirubin ditaurate (TB) is far more stable and is commercially available. Consequently, it has been used as a surrogate for bilirubin diglucuronide in vitro and in animal studies where it was smoothly excreted by the liver.<sup>10</sup>

In solution, a rapid interconversion between the M- and P-helical conformers of the pigments occurs via the breaking and reforming of intramolecular hydrogen bonds. BR binds to deoxycholate micelles,<sup>11</sup> human serum albumin,<sup>12,13</sup> cinchona alkaloid,<sup>14</sup> nucleosides,<sup>2</sup> cyclodextrins (CDx)<sup>15–19</sup> and, in solution, exhibits bisignate Cotton effects detected by means of electronic circular dichroism (ECD) spectroscopy. These effects have been explained by the proposal that the pigment molecule preferably forms one of the diastereoisomers upon complexation with a chiral host. The pigment helical conformer adopts a chiral ‘ridge-tile’ structure, and an exciton coupling between two dipyrrole chromophores splits the excited state of BR into two energy levels leading to a bisignate ECD Cotton effect.<sup>2,12,14</sup> When the orientation of the transition dipoles

\* Corresponding author. Tel.: +420 220443036; fax: +420 220444334; e-mail: [marie.urbanova@vscht.cz](mailto:marie.urbanova@vscht.cz)

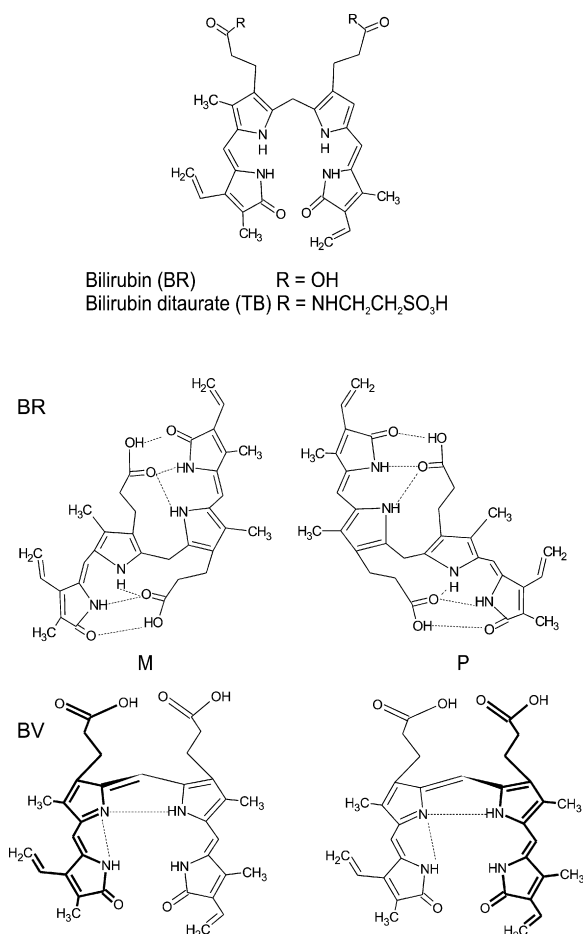


**Figure 1.** Formulas of biliverdin-IX  $\alpha$  (BV), bilirubin-IX  $\alpha$  (BR), and bilirubin ditaurate (TB) showing the interconversion of the intramolecular hydrogen-bonded ridge-tile conformers of bichromophoric BR and the helical enantiomers of BV.

of the two dipyrinone chromophores adopts the M-helix configuration, the ECD spectrum of BR is split into two bands in the wavelength region of the electronic transition, where negative and positive ECD signals appear at longer and shorter wavelengths, respectively, forming a so-called negative couplet. An oppositely signed positive couplet is observed for P-helix BR.

Molecular recognition phenomena involve only noncovalent interactions, such as electrostatic (ion–ion, ion–dipole, dipole–dipole, dipole-induced dipole, and higher order terms), van der Waals, hydrophobic, hydrogen bonding, charge transfer, and  $\pi$ – $\pi$  stacking interactions, and steric effects. It is interesting to note that the weak interactions in general are not sufficient individually to lead to the specific association of two molecules. Usually, molecular association is made possible not by a single weak interaction but through the simultaneous cooperation of several weak interactions.<sup>20</sup> Thus, molecular recognition phenomena may be described as due to the chemistry of cooperative weak interactions. In molecular recognition processes cooperativity plays a central role in controlling the structure and function of the host–guest complexes. An example of such a system is the cyclodextrins, which are widely used for recognition.<sup>20,21</sup> However, they are not flexible enough

to allow allosteric conformational changes. Indeed, in the case of the cyclodextrin inclusion complexes, weak forces that work locally are not always cooperative in nature, but instead may act independently or sometimes even counteract one another. The most important contributions to the complexation of cyclodextrins are believed to originate from the penetration of the hydrophobic part of the guest molecule into the cyclodextrin cavity and hydrogen bonding interactions, which contribute to the stabilization of cyclodextrin complexes with guest molecules.

Lightner et al.<sup>15</sup> reported that BR could be stereoselectively recognized by CDx in water and shows the negative ECD couplet, suggesting that the transition dipoles of the two dipyrinone chromophores of BR take an M-helix configuration. CDx and its complexes have been characterized by spectroscopic methods in reviews.<sup>17,20</sup> When an achiral guest is included in the cavity, induced Cotton effects have been observed by ECD spectroscopy.<sup>22–24</sup> The sign and intensity of the induced ECD signals reflect the orientation of the guest chromophore in the cavity.

Although BR and other derivatized pigments have been studied by various spectroscopic methods, vibrational circular dichroism (VCD) spectroscopy has so far been neglected. VCD spectroscopy is widely used for conformational studies of chiral molecules (see, e.g., Ref. 25–29), and it is also an efficient tool for studying complexes where chiral molecules are involved.<sup>29–32</sup> In VCD spectra, the functional groups participating in complex formation can be assigned on the basis of characteristic vibrations. In a published VCD study<sup>33</sup> of the host–guest binding between CDx and several nonaromatic substances, for example, methyloxirane, 1-propanol, substituted cyclohexanones, copper ions, and also the aromatic compound methyl orange, no noticeable changes in the VCD spectra induced by interactions with nonaromatic compounds have been found; however, significant variations in the VCD patterns have been observed for methyl orange. Setnička et al.<sup>34</sup> reported VCD studies of the inclusion of aromatic compounds into  $\beta$ -,  $\alpha$ -, and  $\gamma$ -CDx complexes and showed changes in the dextrin part of  $\beta$ -cyclodextrin upon inclusion complex formation.

In this paper, we describe a systematic study of diastereodiscrimination of the bile pigments bilirubin, biliverdin, and bilirubin ditaurate by means of two types of  $\beta$ -cyclodextrins: native  $\beta$ -cyclodextrin (CDx) and randomly methylated  $\beta$ -cyclodextrin (MCDx). The main aim of this work is an attempt to elucidate the mechanism of complexation between the pigment stereoisomers and cyclodextrins using ECD and, for the first time, VCD spectroscopy. Taking into account that CDx may serve as an excellent model of an artificial enzyme,<sup>21</sup> spectroscopic studies of the conformational changes of the bile pigments by means of ECD and VCD techniques may help to explain some unknown aspects of pigment metabolism. From a practical point of view, using CDx as a selector is advantageous in the VCD study because the CDx vibrational spectrum does not overlap the BR bands in the mid-IR region and enables identification of a characteristic ‘IR marker’ of the pigment species.

## 2. Results and discussion

### 2.1. Electronic circular dichroism

The left panel of Figure 2 shows the ECD spectra of aqueous solutions of the dianion BR prepared by neutralization of the diacid with NaOH and measured at pH 10.8 in the presence of CDx and MCDx with and without cyclohexanol. While an aqueous solution of pure BR possesses no ECD, the negative couplet induced by CDx or MCDx was observed in agreement with previous reports.<sup>15,16,19</sup> A bisignate ECD spectrum indicates that the dipyrinone moieties of BR bond to CDx selectively and take on an M-helical conformation. Kano et al.<sup>16,18,19</sup> assumed that BR complexes with CDx through a hydrogen bonding interaction between the COO<sup>-</sup> groups of BR<sup>2-</sup> and the secondary hydroxyl groups of CDx and that the absorption of the BR molecule on the CDx outside walls takes place in this case. As for MCDx, the mechanism of complex formation is the same; however, only nonmethylated OH groups are involved in the interaction. This fact explains the weaker signal observed in the BR–MCDx system (cf. curves a and b). Here we anticipate that hydrogen bonds are the only reason for complex formation with stereoselective recognition of the pigment.

Figure 2 also shows the effect of cyclohexanol addition to the systems BR–CDx (curve c) and BR–MCDx (curve d) and the effect of dimethylsulfoxide (DMSO) when used as the solvent (curve f). Addition of cyclohexanol induces a pronounced increase in signal; DMSO used as a solvent produces a significantly diminished ECD signal for BR–CDx. Cyclohexanol forms inclusion complexes with CDx and MCDx<sup>19,20</sup> and, therefore, was used here as a

competitive inclusion agent. The magnitudes of the signals increased upon the addition of cyclohexanol, which serves as a co-existing guest molecule, in accordance with previous observations.<sup>16</sup> This was interpreted as a consequence of an increase in hydrophobicity at the rims of the cyclodextrins, which provide a more favorable environment for hydrogen bond formation between the COO<sup>-</sup> groups of BR<sup>2-</sup> and the secondary OH groups of CDx or MCDx. We suppose also that this condition enables an additional shallow inclusion of BR into the cavities. Our supposition about the inclusion nature of the complexes with BR is supported by the data obtained for the BR–CDx system in DMSO solution.

Although no ECD signal for BR with CDx was observed in DMSO, the results obtained from an <sup>1</sup>H NMR study<sup>16</sup> show the possibility of a hydrogen-bonded complex in DMSO. In this case, hydrogen bonding only, without the inclusion of BR into the CDx cavity, may result in complexation without stereoselectivity. When we used BR in the form of a dianion in our study of the pigment–CDx interaction in DMSO, a weak ECD signal of opposite sign was observed (curve f), which suggests a weak stereoselectivity may be caused by shallow penetration of the BR chromophore into the cavity, permitted by the dissociation of intramolecular hydrogen bonds. As a consequence, intermolecular hydrogen bonds between the COO<sup>-</sup> of BR<sup>2-</sup> and OH of CDx are also formed. Hence, hydrogen bonds solely are not sufficient for stereoselective recognition of BR by CDx. A complex mechanism that involves shallow inclusion into the cyclodextrin cavity and stabilization of the helical conformations formed by means of short-range forces such as hydrogen bonds is necessary for the formation of these complexes.

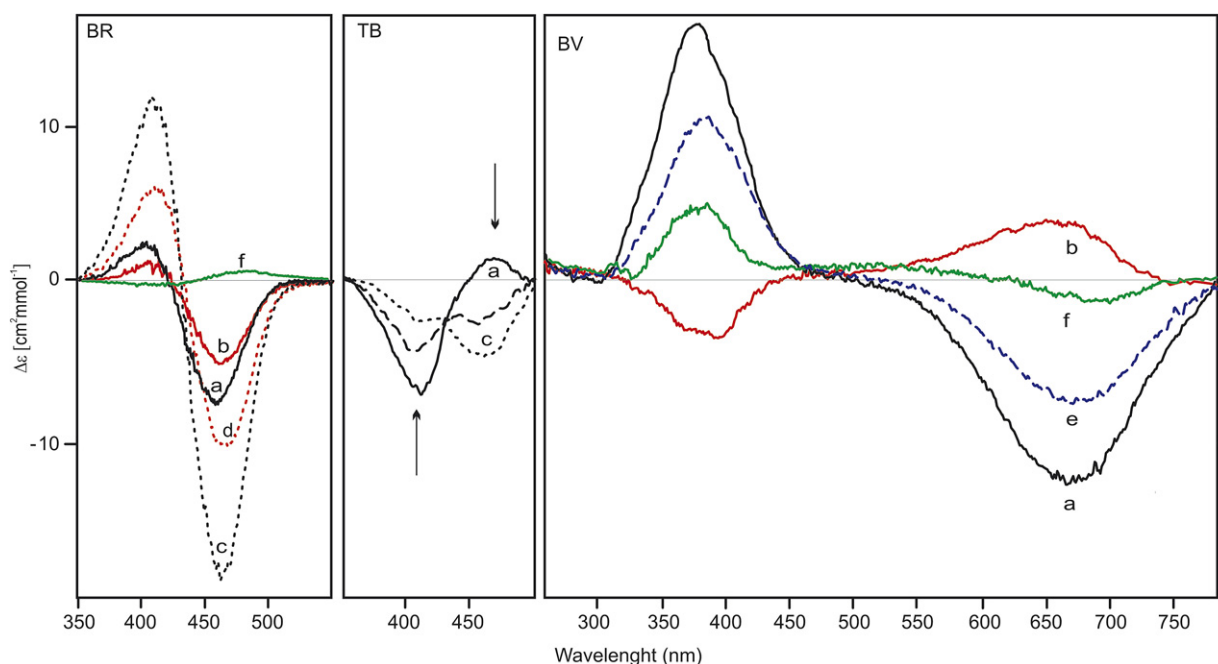


**Figure 2.** ECD spectra of bilirubin (BR), bilirubin ditaurate (TB), and biliverdin (BV) dianions in aqueous solutions with CDx (a), MCDx (b), CDx and cyclohexanol (c), MCDx and cyclohexanol [ $c(\text{cyclohexanol}) = 0.02 \text{ mol L}^{-1}$  (broken line),  $c(\text{cyclohexanol}) = 0.04 \text{ mol L}^{-1}$  (dotted line)] (d), CDx when pigment was added after cyclohexanol addition [ $c(\text{cyclohexanol}) = 0.04 \text{ mol L}^{-1}$ ] (e), and interaction of the pigments with CDx in DMSO (f).  $c(\text{BR}) = 7 \times 10^{-5} \text{ mol L}^{-1}$ ,  $c(\text{BV}) = 7 \times 10^{-5} \text{ mol L}^{-1}$ ,  $c(\text{TB}) = 8 \times 10^{-5} \text{ mol L}^{-1}$ ,  $c(\text{CDx}) = c(\text{MCDx}) = 0.01 \text{ mol L}^{-1}$ .

The middle panel of Figure 2 shows ECD spectra of pure TB dianion in the presence of CDx with and without cyclohexanol. Although TB possesses a conformation in solution that is similar to BR,<sup>10</sup> their ECD signals induced by CDx are reversed (cf. curves a in panels BR and TB). The observed positive couplet at 470(+)/420(–) nm suggests that TB interacts with CDx in the form of a P-helical conformer instead of the M-helical conformer that is formed in the case of the BR–CDx system. The magnitude of the signals is the same for TB with MCDx (spectra not shown) and, as methylation of the OH groups in CDx disrupts hydrogen bonding formation, this shows that it is not the main factor for recognition in this case. Instead, inclusion may be the main reason for stereoselective complex formation in these systems. This observation is consistent with the fact that there are two taurine groups  $\text{NHCH}_2\text{CH}_2\text{SO}_3^-$  in  $\text{TB}^{2-}$  instead of the  $\text{COO}^-$  groups in  $\text{BR}^{2-}$ , and the interaction with the secondary OH groups of CDx is suppressed compared to BR. Gradual addition of cyclohexanol, the competitive inclusion agent, substantially changes the ECD spectrum in the TB–CDx system (curves c, broken and dotted lines). The magnitude of the negative band at 420 nm gradually decreases and a new negative band arises at 470 nm. Finally, two pronounced negative bands, the weaker and the stronger at 420 and 470 nm, respectively, were detected in this case. It follows from the observed induced ECD that the complex is formed in this case, too, but the mechanism is different from the system without cyclohexanol. Addition of cyclohexanol increases the hydrophobicity near the CDx rims, which may cause a weak inclusion of TB chromophores into the cavity and the stabilization of the helical conformation with the help of hydrogen bonding and London forces.

The mechanism of the induction of optical activity in bilirubin and related compounds has been described and discussed in detail.<sup>14</sup> It was shown that monosignate ECD is not characteristic of bichromophore rubin pigments; instead the ECD spectrum of bilirubin is the result of a typical excited state interaction in a weakly coupled electronic system (exciton coupling) and there is no sum of ECD signals independently acted pyrromethone chromophores. The apparent monosignate ECD spectrum of the TB–CDx system obtained in this study may reflect the coexistence of two conformers with different molecular geometries that possess the negative and positive couplets with different intensities. The sum of the couplets leads to the monosignate spectrum observed. Complexation of TB with CDx in DMSO does not show a detectable induced ECD, which can be explained by the fact that: (i) the absence of  $\text{COO}^-$  groups in the  $\text{TB}^{2-}$  structure compared to  $\text{BR}^{2-}$  restricts nonselective complexation via hydrogen bonding to the OH groups of CDx; (ii) the complex formation depends on the dielectric constant of the solvent. The aqueous medium has a higher dielectric constant compared to DMSO and is more likely to favor partial penetration of the pyrromethones into the hydrophobic cavity of CDx.

The right panel of Figure 2 shows the ECD spectra of aqueous and DMSO solutions of BV dianion at pH 10.8

in the presence of CDx and MCDx. Similarly to the other bile pigments, BV alone without CDx or MCDx does not exhibit significant optical activity because it exists as a racemic mixture of two enantiomeric conformers of equal stability in solution.<sup>2,5</sup> BV with CDx shows a strong monosigned positive ECD pattern at 380 nm in the UV region in contrast to the bisignate signal that was observed for BR and TB in this region. While the origin of the optical activity of BV lies in the helical geometry of the single dipyrin chromophore, in the case of BR and TB the bisignate signal is explained by the exciton splitting interaction between two dipyrinone chromophores. In addition, a strong negative ECD pattern was observed at 680 nm in the VIS region (curve a). Using MCDx instead of CDx reverses the signs of both the UV and VIS signals, which simultaneously become weaker (curve b). The structure of BV in the BV–apomyoglobin complex, which possesses negative UV and positive vis patterns, was identified as a P-helical conformation via X-ray.<sup>35</sup> Therefore we interpret our observations as enantioselective recognition of P-helical conformers by MCDx and enantioselective recognition of M-helical conformers by CDx. The spectra obtained are in accordance with previous results in systems with apomyoglobin,<sup>36</sup> amino acids,<sup>7</sup> peptides, and proteins,<sup>6,9,37,38</sup> where induced ECD signals were ascribed as a consequence of the host CDx forcing the guest chromophores to form a chiral conformation. The process of complexation may involve specific intermolecular interactions, mostly electrostatic interactions and hydrogen bonding. We think the crucial factor for chiral discrimination in systems with CDx and MCDx is the entrance of the chromophore into the cavity. Our study has shown that the induced ECD patterns observed for the BV–CDx and BV–MCDx systems are opposite. The observed differences between the ECD spectra of BV in complexes with CDx and MCDx can be correlated with the specific structural characteristics of the two cyclodextrins. In particular, the methylation of the hydroxyl groups in the CDx structure usually leads to an increase in both internal diameters of the cavities.<sup>20</sup> However, in our case, it looks like the presence of  $\text{CH}_3$  groups in MCDx partly prevents BV inclusion (weaker signal), and the P-helical conformation of the pigment in this complex is more favorable. Methylation of the OH groups in the MCDx structure may be the reason for weaker stabilization of the helical conformation of BV due to fewer available hydrogen bonds between OH and  $\text{COO}^-$ . The inverse ECD spectrum of BV–MCDx confirms the inclusion character of the stereoselective complexes, where the different substitutions in the structure of the cyclodextrin groups may affect the preference for one of the two helical conformers. We think the methylation prevents partial inclusion of the pigment chromophore into the cavity.

When cyclohexanol was added to BV–CDx, no significant changes in the shape and magnitude of the ECD spectra were observed. For the MCDx–BV system the signal drastically decreased after cyclohexanol addition and, finally, no ECD signal was observed. When the cyclohexanol–CDx complex was formed first and BV was added later on, a weaker induced ECD signal for BV was observed, which increased in time. The final magnitude of the spectrum was weaker compared to that for the BV–CDx com-

plex without cyclohexanol (cf. curves a and e). For the system MCDx–cyclohexanol, an ECD signal was not obtained after BV addition; therefore, stereoselective complexation does not take place in this case. The induced ECD signal was observed also for the DMSO solution of BV and CDx, suggesting that stereoselective complexation takes place also when hydrogen bonding is suppressed. The experiments with cyclohexanol and DMSO show that the inclusion mechanism is the most important stereoselective factor in BV–CDx complexation and that hydrogen bonds have a stabilizing effect but do not contribute to stereoselectivity. Compared to BR and TB, where inclusion of the chromophores is only shallow and enantioselective complexations are not strong in water and do not take place in DMSO, BV forms enantioselective complexes even in DMSO (curve f).

Further information about the interaction between the pigments and both CDx and MCDx can be deduced from the IR and VCD measurements.

## 2.2. Vibrational circular dichroism

Figure 3 shows the absorption spectra of the pigments studied at pH 10.8 in the range 1800–1500  $\text{cm}^{-1}$  where most of the stretching vibrations of the tetrapyrrole rings can be observed. Matrices of CDx and MCDx do not absorb in this region. Assignment of the infrared bands to the basic functional groups in BR and BV dianions was done according to results reported previously.<sup>39–42</sup> For BR, the broad band at 1670–1600  $\text{cm}^{-1}$  involves three local maxima, 1650, 1630, and 1617  $\text{cm}^{-1}$ , obtained by second derivation. The band at 1650  $\text{cm}^{-1}$  can be assigned to the stretching C=O vibrations, the band at  $\sim 1630 \text{ cm}^{-1}$  is assigned to vinyl coupled lactam and pyrrole ring stretching

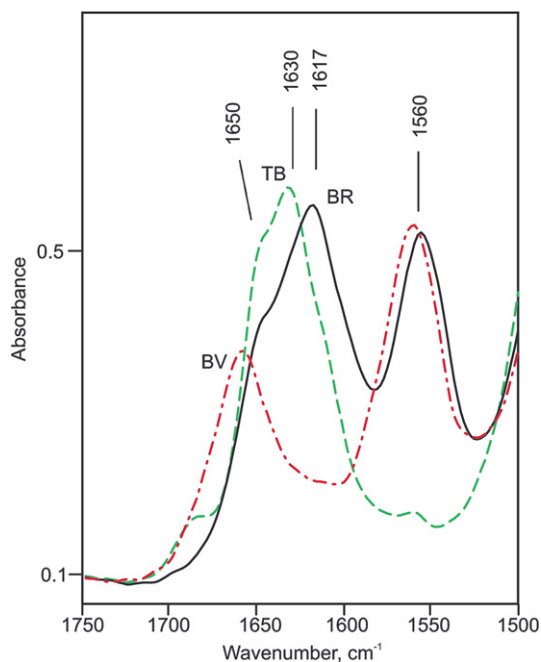


**Figure 3.** Absorption spectra of bilirubin (BR), biliverdin (BV), and bilirubin ditaurate (TB) dianions in aqueous solution.  $\epsilon(\text{pigments}) = 0.08 \text{ mol L}^{-1}$ .

vibrations, and the band near 1617  $\text{cm}^{-1}$  to the pyrrole ring deformation characteristic of molecules possessing intramolecular hydrogen bonds. The broad band may also include the absorption at 1600  $\text{cm}^{-1}$  that was assigned to the vinyl, lactam and bridged C=C stretching vibrations. As for the broad band at 1600–1520  $\text{cm}^{-1}$ , it consists mainly of the asymmetric  $\text{COO}^-$  stretching vibrations of the propionic groups in the  $\text{BR}^{2-}$  structure (1558  $\text{cm}^{-1}$ ) and pyrrole C=C, N–H, and lactam C–N stretching vibrations at 1545  $\text{cm}^{-1}$ .

The absorption spectrum of TB consists of five bands with maxima at 1650, 1631, and 1609  $\text{cm}^{-1}$ , which involve the same vibration modes as the BR band at 1670–1600  $\text{cm}^{-1}$ , and two weak bands at 1690 and 1562  $\text{cm}^{-1}$ . The simultaneous increase in the intensity of the C=O stretching vibrations at 1650  $\text{cm}^{-1}$  and the shift and intensity decrease in the band characteristic of intramolecular hydrogen bonded molecules at 1609  $\text{cm}^{-1}$  indicate fewer intermolecular hydrogen bonds in the dianionic structure of TB in comparison with BR (Fig. 1). The weak band at 1690  $\text{cm}^{-1}$  is a result of pigment aggregation. The weak band at 1560  $\text{cm}^{-1}$  is the pyrrole C=C, N–H, and lactam C–N stretching vibrations, which are located at 1545  $\text{cm}^{-1}$  in the  $\text{BR}^{2-}$  spectrum.

The  $\text{BV}^{2-}$  spectrum possesses two pronounced bands. The band at 1600–1500  $\text{cm}^{-1}$  involves the asymmetric  $\text{COO}^-$  stretching vibration of the propionic groups at 1560  $\text{cm}^{-1}$  and the stretching pyrrole vibrations C=C, N–H, and the lactam vibration C–N at 1545  $\text{cm}^{-1}$ . These vibrations coincide with the analogous vibrations in the BR dianion spectrum. By comparison with  $\text{TB}^{2-}$ , which does not have the  $\text{COO}^-$  groups in its structure and possesses only a very weak band at 1565  $\text{cm}^{-1}$ , the assignment of the broad band centered at 1560  $\text{cm}^{-1}$  as the stretching vibration of the carboxylate groups in BV and BR dianions is corroborated. The second most pronounced band in the BV absorption spectrum is located at 1660 with a shoulder at 1610  $\text{cm}^{-1}$ . It involves the stretching vibrations of C=O and C=C, C=N in the rings. BV does not show the strong band at  $\sim 1620 \text{ cm}^{-1}$  that is characteristic of the stretching vibrations of the pyrrole rings in BR and TB that are involved in intramolecular hydrogen bonds. Its spectrum is in accordance with the specific ‘lock-washer’ conformation with only one or two intramolecular hydrogen bonds compared to presumably four similar bonds for TB and four to six for BR.

Figure 4 shows the VCD spectra of BR and TB dianions in the presence of CDx and MCDx and the influence of cyclohexanol addition to the pigments in the presence of CDx. The solutions of both pigments without cyclodextrins show no VCD signal. Pure CDx and MCDx do not possess a VCD signal in this region either, making them advantageous matrices for VCD study of the conformational changes of tetrapyrroles caused by interactions with chiral agents. For TB dianion in the presence of CDx and MCDx (curves a and b), the positive couplet 1615(+)/1630(–)  $\text{cm}^{-1}$  assigned to vibrations of C=O perturbed by hydrogen bond to the pyrrole rings and stretching vibrations of the vinyl group coupled to the lactam demonstrates

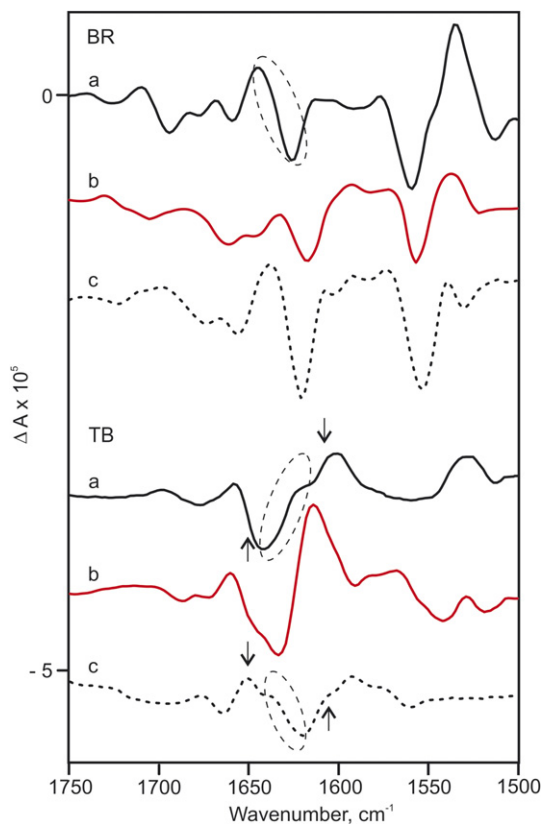


**Figure 4.** VCD spectra of bilirubin (BR) and bilirubin ditaurate (TB) in aqueous solutions at pH 10.8 with CDx (a), MCDx (b), CDx and cyclohexanol (c).  $c(\text{BR}) = 0.08 \text{ mol L}^{-1}$ ,  $c(\text{TB}) = 0.08 \text{ mol L}^{-1}$ ,  $c(\text{CDx}) = 0.075 \text{ mol L}^{-1}$ ,  $c(\text{MCDx}) = 0.12 \text{ mol L}^{-1}$ ,  $c(\text{cyclohexanol}) = 0.06 \text{ mol L}^{-1}$ .

the same specific spatially oriented lactam and pyrrole rings in complexes of TB with both CDx and MCDx at pH 10.8. Addition of cyclohexanol to the CDx–TB system reverses this VCD pattern (cf. curves a and c for TB). In addition, the positive signal at  $1610 \text{ cm}^{-1}$  changes into a negative signal and the negative signal at  $1650 \text{ cm}^{-1}$  turns into a weak positive signal. This supports the opposite arrangement of hydrogen bonded pyrrinone groups in complexes with CDx and in complexes with CDx when cyclohexanol is present. The band at  $1660 \text{ cm}^{-1}$  corresponding to the C=O stretching vibrations observed in the solution without cyclohexanol as a positive signal turns into a negative one when cyclohexanol is added. The VCD observations of TB complexes are in accord with the ECD results that showed significant impact of the presence of cyclohexanol on the spectral pattern (cf. Fig. 2, the middle panel).

For BR, the spectra of the CDx and MDx complexes and of the CDx complex with cyclohexanol show a characteristic positive band in the C=O stretching vibrations region in the lactam rings and a negative couplet  $1620(-)/1640(+)$   $\text{cm}^{-1}$ , which is assigned to the lactam stretching vibrations of C–N and C=C in the hydrogen bonded molecule of BR. These patterns are opposite to the pattern observed for TB with CDx and MDx and similar to the spectral features observed for TB with CDx in the presence

of cyclohexanol. These VCD observations, together with the ECD presented in Figure 2, reflect the fact that the helical conformer recognized when BR complexes with CDx or MCDx is different from the conformer recognized when TB complexes with CDx or MCDx. While the presence of cyclohexanol does not change the sign of the ECD or VCD signals of BR–CDx, the pattern with opposite sign is observed in both ECD and VCD spectra of TB.

Analysis of the obtained VCD results enables us to define the ‘VCD markers’ for the M-helical conformation of BR. The first marker is the negative couplet  $1620(-)/1640(+)$   $\text{cm}^{-1}$ . In addition, the pronounced signal in the region of the antisymmetric  $\text{COO}^-$  stretching vibration at  $\sim 1560 \text{ cm}^{-1}$  can also be considered as characteristic of the M-helical conformation of BR.

Figure 5 shows the VCD spectra of BV dianion with CDx at two concentrations and MCDx. The observed VCD pattern differs significantly from that observed for BR and TB dianions. Three strong negative bands were observed in the presence of CDx. The band at  $1650 \text{ cm}^{-1}$  is assigned to C=O stretching, the band at  $1610 \text{ cm}^{-1}$  to C=N, N–H, and conjugated C=C stretching and the band at  $1560 \text{ cm}^{-1}$  to antisymmetric  $\text{COO}^-$  stretching. Increasing the concentration of CDx while the pigment concentration was kept unchanged was accompanied by an increase in solubility of the complex. Enhancement of the VCD signal in this case implies a shift of the equilibrium toward complex formation. The VCD spectrum of BV in the presence of MCDx roughly shows the opposite sign pattern compared to the BV–CDx spectrum. All the signals are in the

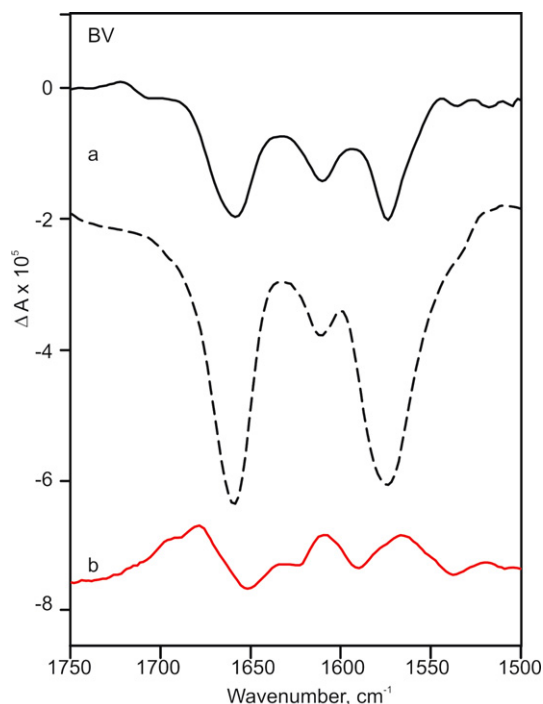


**Figure 5.** VCD spectra of biliverdin (BV) dianion in aqueous solutions with CDx (a),  $c(\text{CDx}) = 0.08 \text{ mol L}^{-1}$  (unbroken line),  $c(\text{CDx}) = 0.14 \text{ mol L}^{-1}$  (broken line), and MCDx (b).  $c(\text{MCDx}) = 0.12 \text{ mol L}^{-1}$ ,  $c(\text{BV}) = 0.08 \text{ mol L}^{-1}$ .

same positions and are weaker than for BV–CDx. The VCD results together with the ECD results imply that CDx and MCDx roughly recognize opposite conformations of BV.

The nature of the interactions of the three bile pigments with the cyclodextrins was further examined using the VCD spectra in the region 1400–1280  $\text{cm}^{-1}$ , which is characteristic of the cyclodextrins,<sup>33,34</sup> and where signals from the pigments are not manifested. Figure 6 shows the VCD spectra of aqueous solutions of pure CDx and CDx with BR, TB, and BV. The VCD spectrum of pure CDx shows bands at 1366(–) and 1327(+) $\text{cm}^{-1}$ , which are assigned to C–O–H and C–H deformations. The two bands are slightly influenced by BR and TB and substantially decreased by interaction with BV. This suggests the different binding mechanisms between BV and CDx on the one hand and BR and TB on the other hand. These kinds of changes in the VCD spectrum of CDx were observed previously<sup>33,34</sup> and were interpreted as being due to the inclusion of an aromatic compound. We observed that small changes in the structure of BV caused different conformations in solution compared to BR and TB and better stereoselective recognition by CDx.

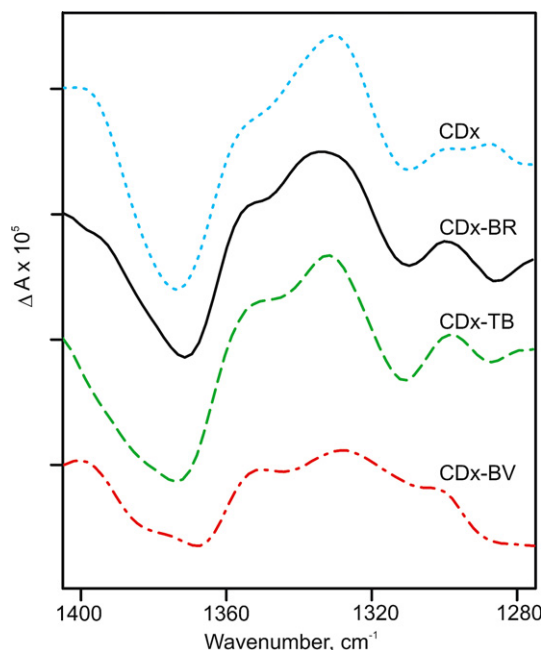


**Figure 6.** VCD spectra of BR, TB, and BV dianions with CDx in aqueous solutions, and aqueous solutions of pure CDx.  $c(\text{pigment}) = 0.08 \text{ mol L}^{-1}$ ,  $c(\text{CDx}) = 0.075 \text{ mol L}^{-1}$ .

### 3. Conclusions

The summarized results described above suggest that unconjugated and conjugated bilirubins have different mechanisms of complexation with cyclodextrins.  $\text{BR}^{2-}$  bonds to CDx and MCDx by means of hydrogen bonds and only shallow inclusion that is restricted by the presence of  $\text{COO}^-$  in the pigment structure. The  $\text{TB}^{2-}$  complex in-

volves weak inclusion of the whole molecule, or some part of it, into the CDx cavity and stabilization of the conformation by hydrogen bonds.  $\text{BV}^{2-}$  forms inclusion complexes and the inclusions are quite deep in this case. The inclusion nature of such complexes can be proved by the weak ECD signal in DMSO where formation of enantioselective complexes via hydrogen bonds is not possible as was shown for BR. The formation of complexes with selective diastereoisomeric preferences and the induced ECD signal for each kind of recognition can be followed by means of electronic as well as vibrational CD spectroscopy. The changes in the region of the VCD spectra where the pigment signals are manifested are reflecting the M-helical stereoisomers of BR and BV and the P-helical conformer of TB. The VCD spectroscopic characteristics of the different conformations were obtained for the first time. The two rubin pigments BR and TB have the same conformation in solution and exist as racemic mixtures of two enantiomeric conformations and, consequently, the pure pigments have neither ECD nor VCD signals, but they can be recognized by CDx or MCDx in the form of opposite conformers. The VCD spectra of these helical conformers are opposite in the region corresponding to the lactam and pyrrole ring stretching vibrations and this characteristic may be used in future VCD studies of BR and TB pigment interactions to provide an explanation of unknown aspects of bile pigment metabolism.

### 4. Experimental

$\beta$ -Cyclodextrin (CDx) (Sigma),  $\beta$ -methylcyclodextrin (MCDx) (Aldrich), and ditaurine amide of bilirubin-IX $\alpha$  disodium salt (bilirubin ditaurate) (Frontier Scientific) were used without further purification. Bilirubin-IX $\alpha$  and biliverdin-IX $\alpha$  hydrochloride (both Frontier Scientific) were used for salt preparation. Double distilled water and DMSO (Sigma) were used as solvents for ECD measurements. VCD spectra were recorded in  $\text{D}_2\text{O}$  (99.9% D, Chemotrade). All other reagents used were of analytical grade.

The disodium salts of the pigments were prepared by freeze-drying methods. Crystalline bilirubin and biliverdin were dissolved in a small excess of NaOH for the full neutralization, intensively shaken, and centrifuged. All manipulations were made rapidly in the dark. The centrifugate was frozen at the temperature of liquid nitrogen and lyophilized with light protection and stored at  $-20^\circ\text{C}$ . Only freshly prepared salts were used during experiments. All the experiments were performed at room temperature and under a nitrogen atmosphere.

The ECD spectra were recorded on a Jasco J-810 spectropolarimeter at room temperature using a quartz cell with a path length of 1 cm, and the samples were flushed with dry ultrapurified nitrogen before and during the experiments. A slit program that afforded wavelength accuracy better than 0.5 nm and integration time of 2 s for each spectral point was used. The pH values of the aqueous solutions were adjusted to 10.8 using  $0.5 \text{ mol L}^{-1}$  NaOH and controlled via a Cole Parmer pH meter with glass microelectrode

(9802BN Orion). No significant change in the pH was confirmed after each measurement. The concentrations of the pigments and CDx (MCDx) were  $7 \cdot 10^{-5}$  and  $0.01 \text{ mol L}^{-1}$ , respectively. The results are presented as mean molecular ECD intensities with respect to total pigment concentration. The concentration used for MCDx was 1.5 times higher than for CDx because of better solubility. Although the VCD patterns for both cyclodextrins are basically the same, the higher concentration used for MCDx caused the features to be more pronounced.

For VCD measurements fresh stock solutions of pigment salts were prepared at concentrations of  $0.16 \text{ mol L}^{-1}$  in  $\text{D}_2\text{O}$  and protected from light. Solutions of the cyclodextrins were prepared at concentrations of  $0.15 \text{ mol L}^{-1}$  (CDx) and  $0.24 \text{ mol L}^{-1}$  (MCDx). The equivalent volume of the pigment stock solution was added to the same volume of the CDx stock solution and the mixture was intensively shaken and protected from light. The final concentrations of the samples prepared were  $0.08 \text{ mol L}^{-1}$  for the pigments and  $0.075$  and  $0.12 \text{ mol L}^{-1}$  for CDx and MCDx, respectively. The pH of the solutions was adjusted to 10.8 using  $\text{NaOD } 0.5 \text{ mol L}^{-1}$  solution in  $\text{D}_2\text{O}$  (Merck). No correction for isotope effects was done.

All samples were allowed to equilibrate for 30 min before the measurements and the stability of the samples was proved by comparison of the infrared absorption spectra recorded before and after each VCD measurement.

VCD spectra were recorded in the  $1800\text{--}1250 \text{ cm}^{-1}$  region at room temperature with a resolution of  $8 \text{ cm}^{-1}$  using a Fourier transform infrared spectrometer IFS-66/S (Bruker, Germany) equipped with a VCD/IRRAS module PMA 37 (Bruker) by a procedure that has been described elsewhere.<sup>43</sup> A demountable cell with the  $\text{CaF}_2$  windows and Teflon spacer of a  $50\text{-}\mu\text{m}$  pathlength was used.

### Acknowledgments

This work was supported by research grants from the Ministry of Education, Youth and Sports of the Czech Republic (MSM 6046137307, OC135) and from Grant Agency of the Academy of Sciences of the Czech Republic (IAA 400550702).

### References

- McDonagh, A. F.; Lightner, D. A. *Cell. Mol. Biol.* **1994**, *40*, 965–974.
- Boiadjev, S. E.; Lightner, D. A. *Tetrahedron: Asymmetry* **1999**, *10*, 607–655.
- McDonagh, A. F.; Lightner, D. A. *Pediatrics* **1985**, *75*, 443–455.
- Mugnoli, A.; Manitto, P.; Monti, D. *Acta Crystallogr., Sect. C* **1983**, *39*, 1287–1291.
- Krois, D.; Lehner, H. *J. Chem. Soc., Perkin Trans. 2* **1993**, 1837–1840.
- Krois, D.; Lehner, H. *J. Chem. Soc., Perkin Trans. 2* **1987**, 219–225.
- Krois, D.; Lehner, H. *Monatsh. Chem.* **1986**, *117*, 1205–1217.
- Haidl, E.; Krois, D.; Lehner, H. *J. Chem. Soc., Perkin Trans. 2* **1985**, 421–425.
- Blauer, G. *Isr. J. Chem.* **1983**, *23*, 201–209.
- Boiadjev, S. E.; Lightner, D. A. *Monatsh. Chem.* **2003**, *134*, 51–59.
- Reisinger, M.; Lightner, D. A. *J. Inclusion Phenom.* **1985**, *3*, 479–485.
- Lightner, D. A.; Reisinger, M.; Landen, G. L. *J. Biol. Chem.* **1986**, *261*, 6034–6038.
- Harmatz, D.; Blauer, G. *Arch. Biochem. Biophys.* **1975**, *170*, 375–383.
- Lightner, D. A.; Gawronski, J. K.; Wijekoon, W. M. D. *J. Am. Chem. Soc.* **1987**, *109*, 6354–6362.
- Lightner, D. A.; Gawronska, J. K.; Gawronska, K. *J. Am. Chem. Soc.* **1985**, *107*, 2456–2461.
- Kano, K.; Imaeda, K.; Ota, K.; Doi, R. *Bull. Chem. Soc. Jpn.* **2003**, *76*, 1035–1041.
- Kano, K. *J. Phys. Org. Chem.* **1997**, *10*, 286–291.
- Kano, K.; Arimoto, S.; Ishimura, T. *J. Chem. Soc., Perkin Trans. 2* **1995**, 1661–1666.
- Kano, K.; Yoshiyasu, K.; Yasuoka, H.; Hata, S.; Hashimoto, S. *J. Chem. Soc., Perkin Trans. 2* **1992**, 1265–1269.
- Connors, K. A. *Chem. Rev.* **1997**, *97*, 1325–1357.
- Tabushi, I.; Shimizu, N.; Sugimoto, T.; Shiozuka, M.; Yamamura, K. *J. Am. Chem. Soc.* **1977**, *99*, 7100–7102.
- Yoshida, N.; Yamaguchi, H.; Iwao, T.; Higashi, M. *J. Chem. Soc., Perkin Trans. 2* **1999**, 379–386.
- Roberts, E. L.; Burguières, S.; Warner, I. M. *Appl. Spectrosc.* **1998**, *52*, 1305–1313.
- Calabro, M. L.; Tommasini, S.; Donato, P.; Stancanelli, R.; Raneri, D.; Catania, S.; Costa, C.; Villari, V.; Ficarra, P.; Ficarra, R. *J. Pharm. Biomed. Anal.* **2005**, *36*, 1019–1027.
- Freedman, T. B.; Long, F. J.; Citra, M.; Nafie, L. A. *Enantiomer* **1999**, *4*, 103–119.
- Keiderling, T. A. *Curr. Opin. Chem. Biol.* **2002**, *6*, 682–688.
- Nafie, L. A.; Freedman, T. B. *Enantiomer* **1998**, *3*, 283–297.
- Nafie, L. A. *J. Phys. Chem. A* **2004**, *108*, 7222–7231.
- Urbanova, M.; Setnicka, V.; Kral, V.; Volka, K. *Biopolymers* **2001**, *60*, 307–316.
- Setnicka, V.; Urbanova, M.; Volka, K.; Nampally, S.; Lehn, J. M. *Chem.-A Eur. J.* **2006**, *12*, 8735–8743.
- Novy, J.; Urbanova, M.; Volka, K. *J. Mol. Struct.* **2005**, *748*, 17–25.
- Palivec, L.; Urbanova, M.; Volka, K. *J. Pept. Sci.* **2005**, *11*, 536–545.
- Bose, P. K.; Polavarapu, P. L. *Carbohydr. Res.* **2000**, *323*, 63–72.
- Setnicka, V.; Urbanova, M.; Kral, V.; Volka, K. *Spectrochim. Acta, Part A* **2002**, *58*, 2983–2989.
- Wagner, U. G.; Muller, N.; Schmitzberger, W.; Falk, H.; Kratky, C. *J. Mol. Biol.* **1995**, *247*, 326–337.
- Marko, H.; Muller, N.; Falk, H. *Monatsh. Chem.* **1989**, *120*, 591–595.
- Krois, D. *Tetrahedron* **1993**, *49*, 8855–8864.
- Braslavsky, S. E.; Holzwarth, A. R.; Schaffner, K. *Angew. Chem., Int. Ed. Engl.* **1983**, *22*, 656–674.
- Yang, B. J.; Taylor, R. C.; Morris, M. D.; Wang, X. Z.; Wu, J. G.; Yu, B. Z.; Xu, G. X.; Soloway, R. D. *Spectrochim. Acta, Part A* **1993**, *49*, 1735–1749.
- Hu, J. M.; Moigno, D.; Kiefer, W.; Ma, J. S.; Chen, Q. Q.; Wang, C. Q.; Feng, H. T.; Shen, J. K.; Niu, F.; Gu, Y. H. *Spectrochim. Acta, Part A* **2000**, *56*, 2365–2372.
- Rai, A. K.; Rai, S. B.; Rai, D. K.; Singh, V. B. *Spectrochim. Acta, Part A* **2002**, *58*, 2145–2152.
- Ferraro, J. R.; Wu, J. G.; Soloway, R. D.; Li, W. H.; Xu, Y. Z.; Xu, D. F.; Shen, G. R. *Appl. Spectrosc.* **1996**, *50*, 922–927.
- Urbanova, M.; Setnicka, V.; Volka, K. *Chirality* **2000**, *12*, 199–203.